Nanoporous Poly(3-alkylthiophene) Thin Films Generated from Block Copolymer Templates

Bryan W. Boudouris,[†] C. Daniel Frisbie,*[,†] and Marc A. Hillmyer*[,‡]

Department of Chemical Engineering and Materials Science and Department of Chemistry, University of Minnesota, Minneapolis, Minnesota 55455

Received July 20, 2007; Revised Manuscript Received October 28, 2007

ABSTRACT: We report the synthesis and characterization of a new series of rod−coil block copolymers, regioregular poly(3-alkylthiophene)-*b*-polylactide (P3AT-PLA), where the alkyl chain in the polythiophene moiety is either 6 or 12 carbons in length. After utilizing a controlled polymerization technique to synthesize end-functionalized P3AT, these polymers were used as macroinitiators for the controlled ring-opening polymerization (ROP) of D,L-lactide. The block copolymers were characterized by ^{1}H NMR spectroscopy, size exclusion chromatography (SEC), differential scanning calorimetry (DSC), thermogravimetric analysis (TGA), wide-angle X-ray scattering (WAXS), ultraviolet−visible (UV−vis) spectroscopy, and atomic force microscopy (AFM). In thin films of these materials (ca. 35 nm thickness), microphase separated domains are formed while the crystallinity of the P3AT majority phase is maintained. Upon chemical etching of the PLA block, we observed a nanopitted film where the crystallinity of the P3AT phase remains; characteristic pits are on the order of 35 nm in diameter with depths of up to 10 nm. The increase in the exposed surface area of the semiconducting polymer (∼150% that of the planar film) could be useful in a variety of organic electronic applications.

Introduction

Poly(3-alkylthiophenes) (P3ATs) have garnered much attention in the organic electronics community due to their high charge transport performance, their chemically tunable electronic properties, and their processability from a variety of solvents.[1−3] Poly(3-alkylthiophenes) are among the leading polymer semiconductors for application in organic field-effect transistors (OFETs),[4−6] volatile organic chemical (VOC) sensors,[7,8] and plastic solar cells.[9−14] Optimizing performance for these applications necessitates precise control of thin film structure,[15−17] and the use of molecular design to control polythiophene thin film morphology continues to be an active area of research. In this report, we describe a novel class of polythiophene-containing block copolymers that can produce a nanoporous P3AT film structure.

Theoretical studies[18−20] have predicted and experimental efforts[21−25] have demonstrated that thin films of diblock copolymers can self-assemble into many types of well-ordered nanostructures on a variety of substrates after being cast from a number of solvents. In most of these cases, both segments of the diblock copolymer contain single-bond carbon−carbon backbone repeat units and thus are considered flexible (or coil-like) in the melt.[26] By selecting the appropriate components of the diblock system, selective etching of the minority phase can lead to nanoporous materials that are useful for applications ranging from separations to templates for nanolithography.[27] In contrast to coil−coil diblock copolymer systems, some polymers contain more rigid backbone bonds that are deemed rodlike in nature, and these are found in many semiconducting polymers, including P3ATs. In a manner similar to their coil-like counterparts, the thermodynamic behavior of rod−coil systems has been investigated both theoretically[28−30] and experimentally.[31−34] While experimental efforts have focused on the phase behavior of rod−coil block copolymer systems and their potential uses in organic electronics applications,[35−44] specific efforts with P3AT block copolymer systems are more uncommon.[7,45−47] This is, in part, because only recently have the synthetic tools become available to generate well-defined P3AT-containing block copolymers.[48]

P3ATs have been traditionally synthesized by electrochemical[49] and oxidative[50,51] polymerizations. However, these resultant polymers tend to be ill-defined with large polydispersities and nonspecific end groups. Recently, the McCullough group showed that highly regioregular, low polydispersity P3ATs could be fabricated via the Grignard metathesis (GRIM) method[52] and that end groups could be controlled via a simple in situ end-capping procedure.[48,53] With the realization of end group control, block copolymers containing P3AT and a more coil-like segment (e.g., polystyrene and poly(methyl acrylate)) have been prepared and tested in organic electronic devices.[45,46,54,55] The addition of the second block not only seems to have an effect on the crystallinity of the materials but also leads to new morphological behavior. Preliminary findings, however, have explored only a handful of insulating moieties and have shown little difference in the thin film microstructure upon changing the second block except in the case of poly(2-vinylpyridine).[46,47,55,56] By expanding the inventory of insulating blocks covalently bonded to the P3AT segment, a better understanding can be gained regarding how the chemical nature of the second block affects P3AT self-assembly. Furthermore, incorporating chemical functionality into the second block allows for the tailoring of thin films that could be useful for enhanced optoelectronic applications.

Polylactide (PLA) has been shown to be a biodegradable and versatile moiety in forming well-ordered block copolymer monoliths and thin films with a variety of morphologies.[57−59] Since the ester linkage in the flexible backbone of the PLA can be selectively etched via a gentle alkaline bath, nanoporous templates with pore sizes on the order of 20 nm can be generated readily in a variety of polymeric matrices without damaging

* Corresponding authors. E-mail: (C.D.F.) frisbie@cems.umn.edu; (M.A.H.) hillmyer@chem.umn.edu.

† Department of Chemical Engineering and Materials Science, University of Minnesota.

‡ Department of Chemistry, University of Minnesota.

10.1021/ma071626d CCC: $40.75
Published on Web 12/06/2007

Table 1. Characterization of P3AT-PLA Samples

sample[a]	M_n[b] (kg/mol) P3AT	M_n[b] (kg/mol) PLA	M_n (kg/mol) total	M_w/M_n[c]	w_{PLA}[d]	T_g (°C)[e] P3AT	T_g (°C)[f] PLA	T_m (°C) P3AT	crystallinity[g] (%)
P3HT-OH	8.0		8.0	1.3		−17		218	18
P3HT(8)-PLA(1)	8.0	0.9	8.9	1.3	0.10	−20	43	223	14
P3HT(8)-PLA(3)	8.0	3.2	11.2	1.3	0.29	−18	42	219	13
P3HT(8)-PLA(31)	8.0	31.0	39.0	1.5	0.79	−21	45	221	12
P3DDT-OH	12.5		12.5	1.3				158	52
P3DDT(13)-PLA(2)	12.5	1.7	14.2	1.4	0.12			149	28
P3DDT(13)-PLA(3)	12.5	2.5	15.0	1.3	0.17			152	26

[a] P3HT-OH is the homopolymer of the poly(3-hexylthiophene)-*b*-polylactide series symbolized by P3HT(*X*)-PLA(*Y*) where the P3HT has a molecular weight of *X* kg/mol and the PLA has a molecular weight of *Y* kg/mol. P3DDT-OH is the homopolymer of the poly(3-dodecylthiophene)-*b*-polylactide series symbolized by P3DDT(*X*)-PLA(*Y*) where the P3DDT has a molecular weight of *X* kg/mol and the PLA has a molecular weight of *Y* kg/mol. [b] As determined by ^{1}H NMR spectroscopy. [c] As determined by SEC vs polystyrene standards. [d] $w_{PLA} = M_n(PLA)/[M_n(PLA) + M_n(P3AT)]$. [e] The glass transition temperature of P3DDT was not prominent enough to be observed in either the homopolymer or diblock copolymers of the series. [f] A broad peak associated with the side-chain melting of the P3DDT samples hindered the appropriate identification of the PLA glass transition temperature in the P3DDT series. [g] As determined by the ratio of the enthalpy of melting for the P3AT fraction of the sample relative to the infinite enthalpy of melting reported in the literature for the P3AT (see discussion in the text).

the matrix material.[27,60,61] In P3AT-containing block copolymers, distinguishing the spatial regimes of the amorphous component of the P3AT block from the coil-like second block via direct imaging techniques can be difficult. By using a block that can be selectively etched, topological changes in the film before and after etching (e.g., using atomic force microscopy) can be monitored and can help reveal the thin film structure.

In this paper we report the stepwise synthesis of poly(3-alkylthiophene)-*b*-polylactide block copolymers (P3AT-PLA) by the controlled polymerization of D,L-lactide[62−64] from hydroxyl-terminated poly(3-alkylthiophenes) (P3AT-OH) which form microphase separated thin films with domains on the order of 30 nm. The PLA can be selectively etched from the films leading to P3AT films with high porosities. Nanoporous P3AT films could lead to enhanced performance of organic electronic devices such as sensors and solar cells. For example, the porous-P3AT film could lead to better sensitivity in detection of VOC vapors in field-effect transistor devices. Also, pitted P3AT block copolymer films could be backfilled with an electron-accepting material, such as buckminsterfullerene (C_{60}), and the enhanced P3AT/C_{60} contact may facilitate better exciton dissociation and charge collection in ordered bulk heterojunction solar cells.[65,66] These possibilities have motivated our efforts to develop strategies that lead to nanoporous P3AT films.

Experimental Section

General Methods. The ^{1}H NMR spectra were measured on a Varian VI-500 spectrometer using deuterated chloroform (Cambridge) solutions containing ∼1 wt % polymer. Size exclusion chromatography (SEC) data were collected on a Hewlett-Packard 1100 series equipped with a Hewlett-Packard 1047A refractive index (RI) detector and three Jordi poly(divinylbenzene) columns of 10^4, 10^3, and 500 Å pore sizes. Tetrahydrofuran (THF) at 40 °C was used as the mobile phase at a flow rate of 1 mL/min and the SEC was calibrated with polystyrene standards (Polymer Laboratories). Differential scanning calorimetry (DSC) measurements were acquired using a TA Q1000 calorimeter. The samples were first annealed at +250 °C and then cooled to −50 °C at a rate of 10 °C/min. The results shown are for the final sample heating at a rate of 10 °C/min. An indium standard was used to calibrate the instrument and nitrogen was used as the purge gas. Thermogravimetric analysis (TGA) was performed with a Perkin-Elmer TGA 7 in a nitrogen atmosphere with a heating rate of 10 °C/min. Wide-angle X-ray scattering (WAXS) data were collected in the diffraction angular range of 3−30° (2θ) by a Bruker-AXS D5005 microdiffractometer. The crystalline peaks were referenced from known reflection values[67] and deconvoluted using the curve-fitting software, JADE 7 (CMI). Film thicknesses were estimated by scratching the polymer film and measuring the step change with a KLA-Tencor P16 profilometer. Ultraviolet−visible (UV−vis) absorption spectra of polymer thin films were taken on a Spectronic Genesys 5 spectrometer over a wavelength range of 300−900 nm using a bare ITO-coated glass substrate as a blank. Atomic force microscopy (AFM) images were taken with a Veeco Metrology Nanoscope IIIa microscope operating in tapping mode.

Materials. All reagents and solvents were used as received from Sigma-Aldrich unless otherwise noted. Degassed THF and toluene were purified by passage through an activated alumina column and were collected in flame-dried, air-free flasks. D,L-Lactide was purified by recrystallization from ethyl acetate followed by drying under reduced pressure and was stored in an inert atmosphere glovebox.

Synthesis of Hydroxyl-Terminated Poly(3-alkylthiophene) (P3AT-OH). A modified method similar to that of the McCullough group was used for the synthesis of hydroxyl-terminated poly(3-alkylthiophene)s.[54] A typical polymerization is described for the hydroxyl-terminated poly(3-dodecylthiophene) (P3DDT-OH) (Table 1). The polymerization was performed in a flame-dried 250 mL reaction flask containing a Teflon-coated magnetic stir bar. To the flask, ∼150 mL of anhydrous THF was added via cannula. 2,5-dibromo-3-dodecylthiophene (6.6 g, 16 mmol) and a solution of 1 M *tert*-butylmagnesium chloride in THF (16 mL, 16 mmol) were added to the THF solvent under N_2. The reaction was placed in an oil bath and heated to reflux for 1.5 h. After cooling the solution to room temperature, 1,3-bis(diphenylphosphino)propane nickel(II) chloride [Ni(dppp)Cl_2] (0.098 g, 0.18 mmol) was added as a solid under N_2 and the reaction was allowed to stir for 1 h. A solution of 1 M vinylmagnesium bromide in THF (3 mL, 3 mmol) was added under N_2 and the reaction was allowed to stir for 1 h prior to precipitation in methanol. The polymer was collected and purified via Soxhlet extraction with methanol, hexane, and chloroform, sequentially. The concentrated chloroform fraction was precipitated in methanol and the vinyl-terminated poly(3-dodecylthiophene) (P3DDT-vinyl) was washed with methanol, collected, and dried overnight under reduced pressure.

The reaction to convert the P3DDT-vinyl end groups to hydroxyl end groups was carried out in a flame-dried 250 mL reaction flask containing a Teflon-coated magnetic stir bar. After flame-drying, 80 mL of anhydrous THF was added via cannula. P3DDT-vinyl (0.8 g, 0.06 mmol) and a 0.5 M solution of 9-borobicyclononane (9-BBN) in THF (13 mL, 6.5 mmol) were added to the reaction flask under N_2. The flask was placed in an oil bath and heated to 45 °C for 24 h. At this point, 6 M NaOH in deionized water (8 mL, 48 mmol) was added to the reaction flask under N_2. The reaction was cooled to room temperature and a 30 wt % hydrogen peroxide aqueous solution (Mallinckrodt Chemicals, 8 mL) was added to the reaction flask. Heat was reapplied and the solution was allowed to stir at 45 °C for 24 h. The reaction was then cooled to room temperature and precipitated in methanol. The polymer was filtered, washed with methanol and deionized water, and dried under vacuum overnight.

Characterization of a Representative P3HT-OH. ^{1}H NMR (500 MHz, $CDCl_3$): δ_H 0.9 (t, 3H), 1.3 (m, 6H), 1.7 (t, 2H), 2.8 (t, 2H), 3.0 (t, 2H), 3.9 (m, 2H), 6.9 (s, 48H). SEC: M_n = 12100; PDI = 1.3.

Characterization of a Representative P3DDT-OH. ^{1}H NMR (500 MHz, $CDCl_3$): δ_H 0.9 (t, 3H), 1.3 (m, 18H), 1.7 (t, 2H), 2.8 (t, 2H), 3.0 (t, 2H), 3.9 (m, 2H), 6.9 (s, 50H). SEC: M_n = 18900, PDI = 1.3.

Synthesis of Poly(3-alkylthiophene)-*b*-polylactide (P3AT-PLA). Macroinitiated ring-opening polymerizations of lactide are well-known, and we have used a method similar to one previously reported for the polymerization of lactide using hydroxyl-terminated polystyrene as the macroinitiator.[68] The details for the example polymerization of P3DDT(13)-PLA(2) are as follows. P3DDT-OH (0.161 g, 0.013 mmol) was dried under reduced pressure in a reaction flask at 110 °C for 24 h. The flask was then sealed and transferred inside of a glovebox where toluene (1.4 mL) was used to dissolve the P3DDT-OH. A solution of 1 M triethyl aluminum ($AlEt_3$) in toluene (13 μL, 0.013 mmol) was also added in order to have equal molar amounts of $AlEt_3$ and P3DDT-OH present to form the macroinitiator. The reaction was then sealed and brought outside the glovebox to be placed in an oil bath at 90 °C for 16 h. At this point, the reaction mixture was cooled and transferred back inside the glovebox, and D,L-lactide (0.21 g, 1.4 mmol) was added. The reaction was capped and returned to the oil bath where it was heated at 90 °C for an additional 5 h. The reaction was cooled to room temperature, quenched with ~2 M HCl (1 mL, 2 mmol), and precipitated in methanol. After filtering and washing with methanol, the polymer was dried overnight under vacuum.

Characterization of P3HT(8)-PLA(1). ^{1}H NMR (500 MHz, $CDCl_3$): main chain P3HT peaks are the same as for P3HT-OH with δ_H 1.6 (m, 3H), 3.1 (t, 2H), 4.3 (m, 3H), 5.2 (m, 14H). SEC: M_n = 12500; PDI = 1.3.

Characterization of P3HT(8)-PLA(3). ^{1}H NMR (500 MHz, $CDCl_3$): main chain P3HT peaks are the same as for P3HT-OH with δ_H 1.6 (m, 3H), 3.1 (t, 2H), 4.4 (m, 3H), 5.2 (m, 45H); SEC: M_n = 12900; PDI = 1.3.

Characterization of P3HT(8)-PLA(31). ^{1}H NMR (500 MHz, $CDCl_3$): main chain P3HT peaks are the same as for P3HT-OH with δ_H 1.6 (m, 3H), 3.1 (t, 2H), 4.4 (m, 3H), 5.2 (m, 430H). SEC: M_n = 15000; PDI = 1.5.

Characterization of P3DDT(13)-PLA(2). ^{1}H NMR (500 MHz, $CDCl_3$): main chain P3DDT peaks are the same as for P3DDT-OH with δ_H 1.6 (m, 3H), 3.1 (t, 2H), 4.4 (m, 3H), 5.2 (m, 27H). SEC: M_n = 21200; PDI = 1.4.

Characterization of P3DDT(13)-PLA(3). ^{1}H NMR (500 MHz, $CDCl_3$): main chain P3DDT peaks are the same as for P3DDT-OH with δ_H 1.6 (m, 3H), 3.1 (t, 2H), 4.4 (m, 3H), 5.2 (m, 35H). SEC: M_n = 21900; PDI = 1.3.

P3AT Series Thin Film Preparation. Solutions of P3AT-OH and P3AT-PLA were made by dissolving 20 mg of polymer in 1 mL of 1,2-dichlorobenzne (DCB) and allowing the solutions to stir at 60 °C under inert atmosphere overnight. ITO-coated glass substrates (Delta Technologies) were sonicated for 10 min sequentially in acetone, chloroform, and isopropanol and dried with compressed N_2. Solutions were passed through a 0.45 μm syringe filter and spun-cast onto the substrates using the slow-drying technique developed by Li et al.[11] The solutions were deposited on the substrates and the rotation rate was increased from 0 to 700 rpm over the course of ~2 s and held at 700 rpm for 60 s. The wet films were then transferred to a Petri dish and covered to allow for slow evaporation of the DCB, which led to drying times on the order of 1 h. After the films were dry, they were transferred into inert atmosphere and annealed for 1 h at 165 °C. The thicknesses of all of the films, as measured by profilometry, were 37 ± 4 nm.

Etching of the P3AT Series Thin Films. As described previously, a 0.5 M solution of NaOH in water/methanol (60/40 v/v) was used to etch the PLA moiety from the block copolymer thin films.[57] The samples were etched for up to 72 h at room temperature and were then washed with deionized water and dried with compressed N_2. The removal of PLA was monitored by ^{1}H NMR spectroscopy.

Scheme 1. Synthesis of Poly(3-alkylthiophene)-*b*-Polylactide Copolymers

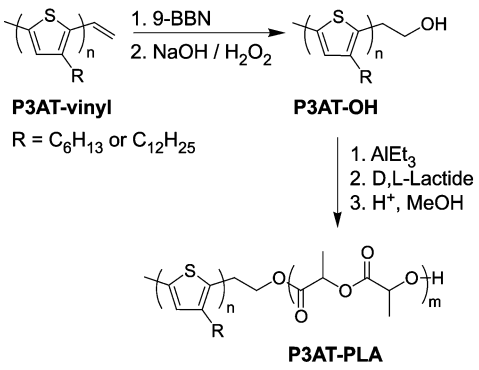

Results and Discussion

Synthesis of P3AT-PLA. The new method for synthesizing P3AT block copolymers that contain PLA is shown in Scheme 1. The first step in forming these block copolymers was to generate vinyl-terminated poly(3-alkylthiophene) homopolymers. These polymers were synthesized using the Grignard metathesis (GRIM) method and subsequent end-capping with vinyl magnesium bromide.[48] Soxhlet extractions can be used to fractionate P3ATs.[69,70] To remove small molecular weight polymers and any residual reagents from the polymerization reaction, the polymers were Soxhlet extracted with methanol, hexane, and chloroform in a sequential manner. In the chloroform fraction of the P3AT-vinyl polymers there was not complete addition of the vinyl group to the end of the polymer chains for the P3HT-vinyl (~92% functionality) and P3DDT-vinyl (~95% functionality) precursors. This causes a small amount of residual P3AT homopolymer to be present in all of the samples discussed below. The chloroform fraction of the vinyl-terminated polymers (P3AT-vinyl) was then converted to hydroxyl-terminated poly(3-alkylthiophenes) (P3AT-OH) via hydroboration and oxidation of the end group in a process similar to that described by the McCullough group.[54] The P3AT-OH homopolymers exhibited narrow molecular weight distributions (M_w/M_n = 1.3) by SEC (Table 1) which is typical for polymers synthesized via the GRIM method.[71] These P3AT-OH homopolymers were used as controls in the block copolymer thin film studies described below and were also the starting materials for the synthesis of P3AT-PLA.

The use of aluminum alkoxide initiators to create polylactide with a narrow molecular weight distribution via ring-opening polymerizations (ROPs) has been studied previously.[62−64] In the current system, triethylaluminum was used to convert the P3AT-OH to the corresponding aluminum alkoxide macroinitiator. It was this macroinitiator that was used in the ring-opening polymerization of D,L-lactide to yield the atactic form of PLA.[72] By varying the conversion of lactide, the molecular weight of the PLA block was controlled (Table 1).

Molecular Characterization of P3AT-PLA. To observe the conversion of P3AT-vinyl to P3AT-OH and P3AT-OH to P3AT-PLA, ^{1}H NMR spectroscopy was used to monitor the resonances of the end groups associated with each of these three types of polymers. The molecular weights of the P3AT-OH homopolymers were determined by ^{1}H NMR spectroscopy using end group analysis, and these molecular weights were used in all further computations. Calculations were based on NMR determined molecular weights due to the fact that SEC calculated

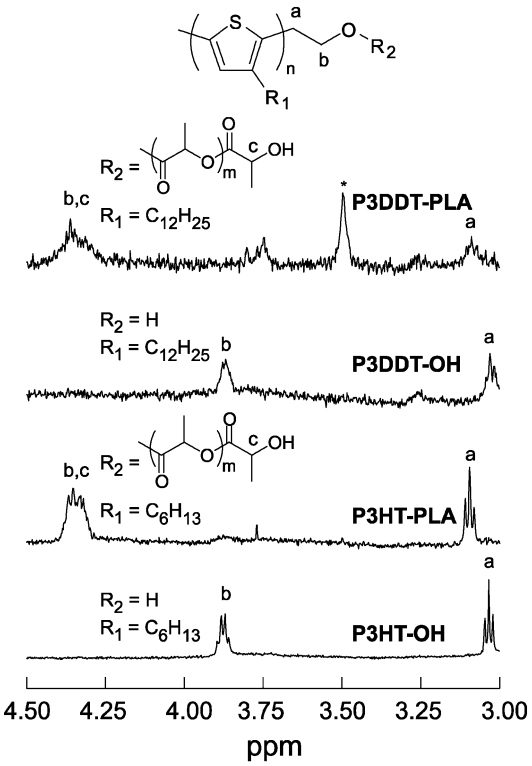

Figure 1. ^{1}H NMR spectra of P3HT-OH and a representative block copolymer for the P3HT-PLA series along with the ^{1}H NMR spectra of P3DDT-OH and a representative block copolymer for the P3DDT-PLA series. All polymers were dissolved in $CDCl_3$. The asterisk at ~3.5 ppm in the P3DDT-PLA spectrum is a signal due to residual methanol present in the sample.

molecular weights of rodlike polymers (specifically polythiophenes) vs polystyrene standards can overestimate the true molecular weight of the polymer by over a factor of 2.[73] By observing the chemical shifts and splitting patterns in the spectra we are able to see full conversions of the P3AT-OH to P3AT-PLA (Figure 1). In both the P3HT and P3DDT cases, there is a clear shift of both of the methylene resonances (a and b in Figure 1) upon the addition of polylactide along with the appearance of resonances associated with the terminal repeat unit of the PLA moiety. The presence of peaks at 3.0 and 3.9 ppm for the P3AT-OH end groups were in good agreement with previous reports.[54] The appearance of the peak at 4.4 ppm upon the addition of PLA was consistent with the terminal lactide repeat unit and appears at the same chemical shift as the methylene protons between the P3AT and PLA chains (b in Figure 1).[74] Additionally, integration of the area under the end group peaks before and after lactide polymerizations were in good agreement with the predicted structures.

Figure 2 shows the entire ^{1}H NMR spectra of a representative P3AT-PLA block copolymer with the resonances of backbone atoms in PLA (b and c). The areas under these peaks were integrated and the relative intensities were compared with the already determined main-chain resonances associated with the P3AT segment (a) to gauge the molecular weight of the PLA segment. Because of the relatively high molecular weight of P3AT present in this sample, the end group peaks shown in Figure 1 are not clearly visible in the full ^{1}H NMR spectrum.

The molecular weight distributions of the homopolymer and diblock copolymer materials were evaluated by SEC, and the results show a general trend of constant or slightly increasing polydispersity with the length of the PLA chain. This is consistent with the concepts of the equilibrium polymerization

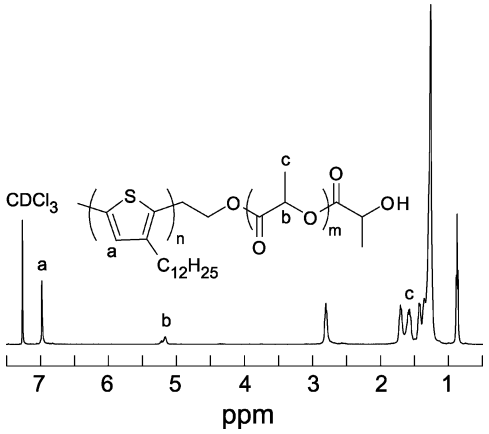

Figure 2. ^{1}H NMR spectrum of a representative block copolymer, P3DDT(13)-PLA(2), in $CDCl_3$. The unlabeled peaks upfield of 3.5 ppm are associated with the dodecyl side chain of this polymer.

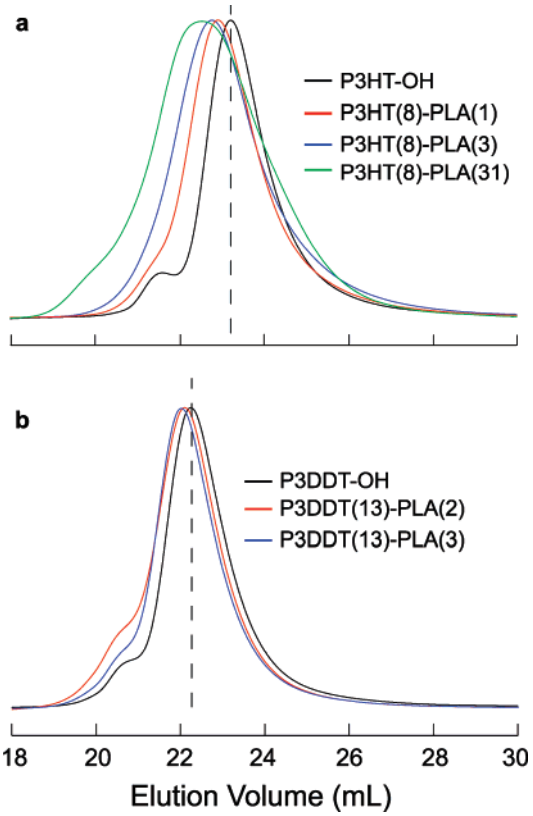

Figure 3. SEC traces of the (a) P3HT-PLA series and (b) P3DDT-PLA series with THF as the mobile phase. Dashed lines are guides for the eye through the apex of the SEC trace of the P3AT homopolymer chromatogram.

and growing polydispersities with growing reactions times for the PLA moiety.[75] In addition to monitoring the polydispersities of the block copolymers SEC traces show clear, monomodal distributions after the addition of the PLA block, reaffirming the results offered by end group integration, which suggest all PLA present in the samples is covalently bound to the P3AT chains (see Figure 3). We believe the small shift in elution volume reflects the rod−coil nature of P3AT-PLA type polymers. Since the addition of a short, flexible PLA block only slightly impacts the overall hydrodynamic volume of the rather rigid and bulky P3AT segment, shifts in retention volume are smaller than would be expected for a coil−coil system but are still clear and consistently shifted to lower elution volumes as the molecular weight of the PLA moiety is increased.

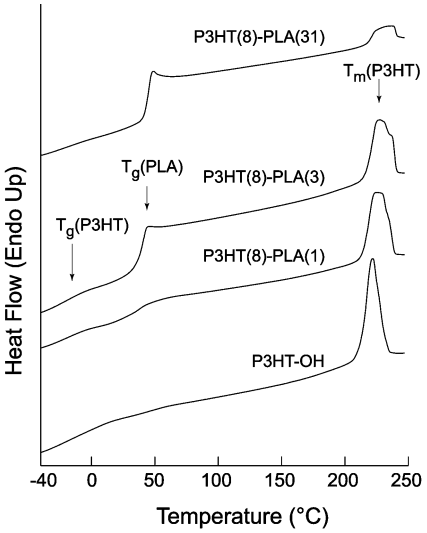

Figure 4. DSC traces of P3HT-PLA series at 10 °C/min showing the separate glass transitions for P3HT, PLA, and the melting temperature of P3HT.

Thermal Characterization of P3HT-PLA. The polymers were subjected to DSC analysis in order to observe the melting points and glass transitions of the materials, gauge the crystallinity of the P3AT segments, and verify the presence of microphase separated domains. The appearance of distinct glass transition temperatures for P3HT ($T_g \sim -20$ °C) and PLA ($T_g \sim 43$ °C) (Figure 4), which are consistent with literature values, support P3AT-PLA microphase separation.[76−78] The amount of polymer that was crystalline in the sample was determined by integrating the area under the melting peak in each of the three samples, normalizing the values by the amount of P3HT present in the sample, and comparing this with the literature value for the enthalpy of fusion for an ideal P3HT crystal, $\Delta H_m^\infty = 99$ J/g.[79] Since the atactic PLA is prevented from being included in the crystalline matrix, the existence of PLA in the block copolymer slightly lowers the amount of crystallinity in the diblock copolymers vs the homopolymer (see Table 1). One concern observed during the course of these measurements was the relatively high melting temperature ($T_m \sim 220$ °C) of the P3HT segment.[79−81] Previous reports have indicated that thermal degradation of PLA occurs at or below 220 °C.[57]

Thermal Characterization of P3DDT-PLA. To avoid the possible thermal degradation problem associated with the P3HT-based diblock copolymers, the P3DDT series was synthesized, since it is well-known that the melting temperature of P3ATs decreases as the length of the alkyl chain is increased.[82,83] As previously seen in the literature, P3DDT has two melting transitions. The first is a broad peak spanning 25−80 °C and is associated with the melting of ordered alkyl groups in the material due to the high regioregularity of the polymer and the rather long side chains.[84] Due to the broadness of the signal related to the side chain melting of the P3DDT, discerning the glass transition of the PLA was difficult. The main chain melting peak ($T_m \sim 150$ °C) occurs at a much lower temperature than that of P3HT and the value of ΔH_m^∞ is much smaller at 55 J/g.[79] The multiple signals present in the main chain melting peak of the P3DDT, are consistent with previous literature accounts and have been attributed to a combination of melting processes.[79,82] The amount of crystallinity present in the P3DDT homopolymer was much greater than that of the P3HT homopolymer, but the addition of the PLA segment had the same qualitative effect on the crystallinity of the diblock copolymers in the series. With the melting temperature of the P3DDT block being lower than the degradation temperature of PLA, thermal processing of these diblock copolymers is more tractable.

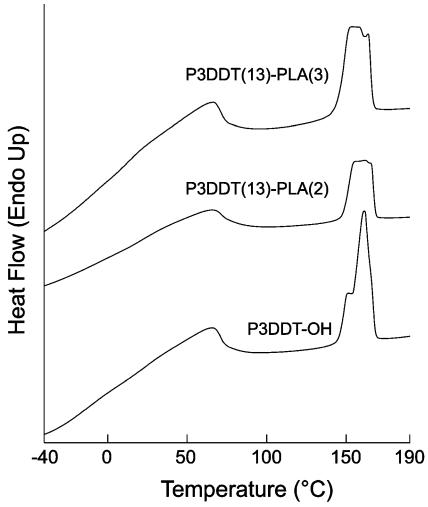

Figure 5. DSC traces of P3DDT-PLA series at 10 °C/min showing the broad side-chain relaxation process for P3DDT and the melting temperature of P3DDT. The glass transition of PLA is obscured for all samples due to the side-chain relaxation of P3DDT.

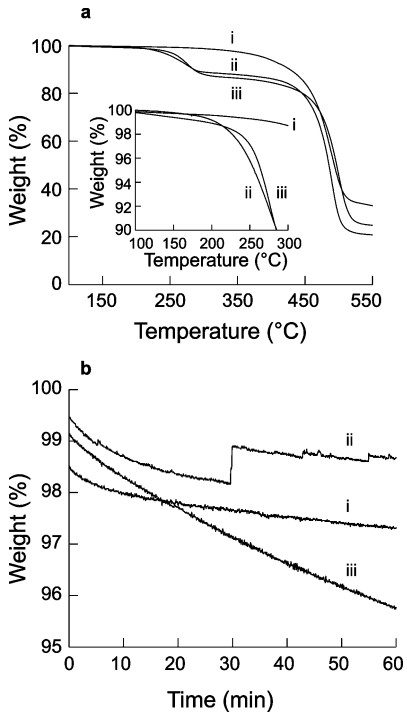

Figure 6. (a) Weight loss with respect to temperature of (i) P3DDT-OH, (ii) P3DDT(13)-PLA(2), and (iii) P3DDT(13)-PLA(3) in nitrogen at a heating scan rate of 10 °C/min. The inset highlights the large amount of weight loss in the block copolymers around the melting temperature of P3HT. (b) Weight loss with respect to time of (i) P3DDT-OH, (ii) P3DDT(13)-PLA(2), and (iii) P3DDT(13)-PLA(3) at a constant temperature of 165 °C in nitrogen. The P3DDT(13)-PLA-(2) trace shows some noise at ∼30 min due to a jostling of the instrument.

In order to verify the ability of the P3DDT-PLA to be processed above the melting temperature of the semiconducting segment, thermogravimetric (TGA) measurements were performed to observe the onset of PLA degradation in these polymers. As shown in Figure 6a, the onset of PLA degradation begins at ∼200 °C with nearly all of the PLA degraded by 280 °C. The midpoint of the weight loss plateau regions of P3DDT(13)-PLA(2) and P3DDT(13)-PLA(3) are at 87% and

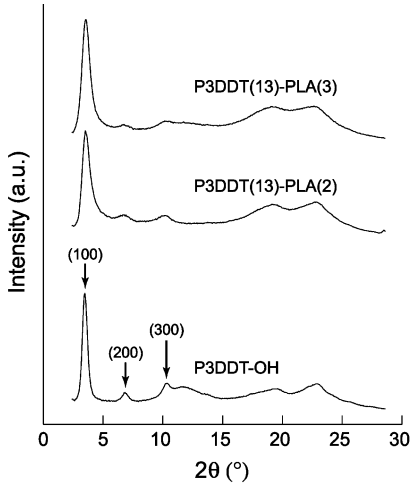

Figure 7. WAXS patterns of the P3DDT-PLA series with arrows showing the first three lamellae reflections of the homopolymer.

82%, respectively, which corresponds well with the weight fraction of PLA in the block copolymers (see Table 1). Figure 6b shows the effect of holding the P3DDT-PLA polymers at ~10 °C above the melting temperature of the P3DDT for 1 h. While there is some noise due to the relatively small window of weight fraction plotted, processing the polymers above the melting temperature of P3DDT will not cause significant degradation of PLA over the course of the experiment. Despite the fact that P3HT outperforms P3DDT in charge transport measurements, we performed all structural and thin film experiments on the P3DDT-PLA series for this reason.[85,86]

Wide-Angle X-ray Scattering (WAXS). WAXS was employed to observe the effect of the PLA block on the crystallinity of P3DDT. The signal at lower scattering angles is indexed as the (100) reflection and is associated with the layered structure of the P3DDT main chain folding into the crystalline matrix. Since the lamellae of the P3DDT structure is known to be significant and that the packing is highly interdigitated, the (200) and (300) reflections are also prominent in the homopolymer chains.[82,87,88] This high degree of ordering leads to a large fraction of crystalline domains in the polymer (also reflected by the DSC measurements). Since the P3DDT alkyl side chains are rather long, they can interpenetrate the overlaying lamellae structure of the main chain and this is the cause for the side chain crystallization (melting) observed in the DSC thermograms. As PLA was incorporated into the block copolymers the crystalline peaks remained but were broadened due to the incorporation of the amorphous PLA domains.

Ultraviolet−Visible (UV−Vis) Light Absorbance. P3AT thin films are often used as the primary light absorbers and electron donors in organic photovoltaic devices.[10,11] For the block copolymers to be useful in this application they must absorb light as the P3AT homopolymers do. We show the results of increasing the amount of PLA relative to P3DDT in the block copolymer samples and the corresponding decrease of light absorption in the wavelength range of 400−600 nm. In order to help induce organization of the P3DDT chains during the spin-coating process, the slow-drying technique developed by Li et al. was used.[11] This slow casting procedure leads to reasonably well-ordered films even prior to annealing since the slow drying of the 1,2-dichlorobenzene (over the course of ~1 h) gives the polymer chains sufficient time to organize prior to locking into a semicrystalline structure (Figure 8a). As expected, decreasing the amount of P3DDT in the sample decreases the relative amount of light absorbed. Despite the fact that the

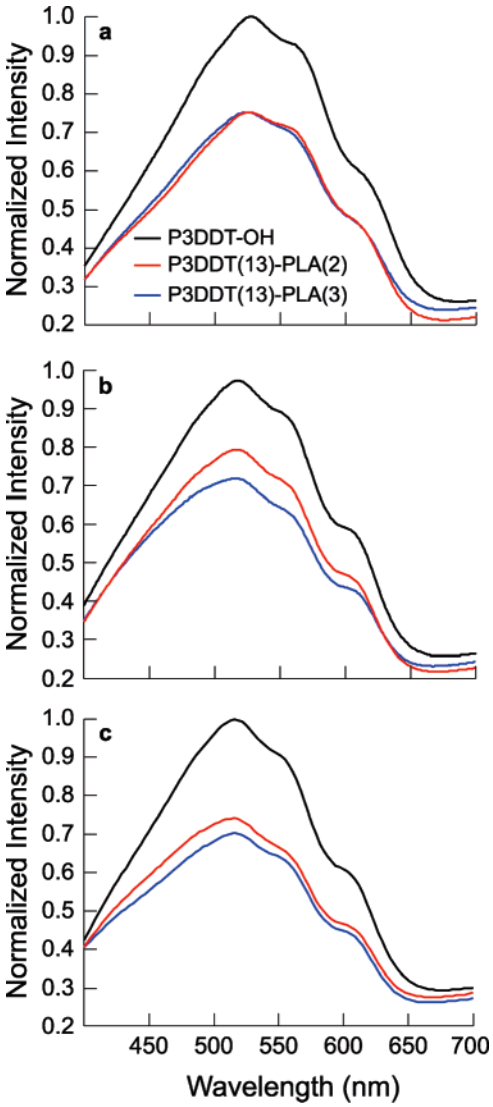

Figure 8. UV−vis absorbance spectra of P3DDT-PLA series thin films (a) as-spun from 1,2-dichlorobenzene, (b) after annealing in inert atmosphere, and (c) after etching the films in a solution of 0.5 M NaOH in water/methanol (60/40 v/v) for 72 h to selectively remove the PLA segment from the diblock copolymers.

absorbencies of the block copolymer films were lower than that of the homopolymer, spectra of all films showed three maxima over the range of P3DDT absorption. The shoulder at ~625 nm is related to vibronic absorption and is an indicator that there a high degree of ordering in both the homopolymer and block copolymers despite the presence of the amorphous PLA.[89] Annealing of the films in inert atmosphere leads to a slight increase in absorption for the block copolymer thin films relative to the homopolymer as the polymer chains are given more of an opportunity to reorganize into an ordered structure (Figure 8b). In addition, a blue shift in the main absorbance peak of the homopolymer and block copolymer films is seen upon annealing. The shift between the as-spun and annealed films is likely due to the relatively rapid cooling of the annealed film as compared to the slower solvent evaporation in the spin-coating process. The longer solvent annealing process presumably leads to a more organized structure and concomitant shift of the principal absorption to a longer wavelength. After chemical etching of the films (see Experimental Section), the absorbance spectrum of the homopolymer and block copolymers remains unchanged, consistent with the idea that the sacrificial PLA block is selectively etched while leaving the semicrystalline

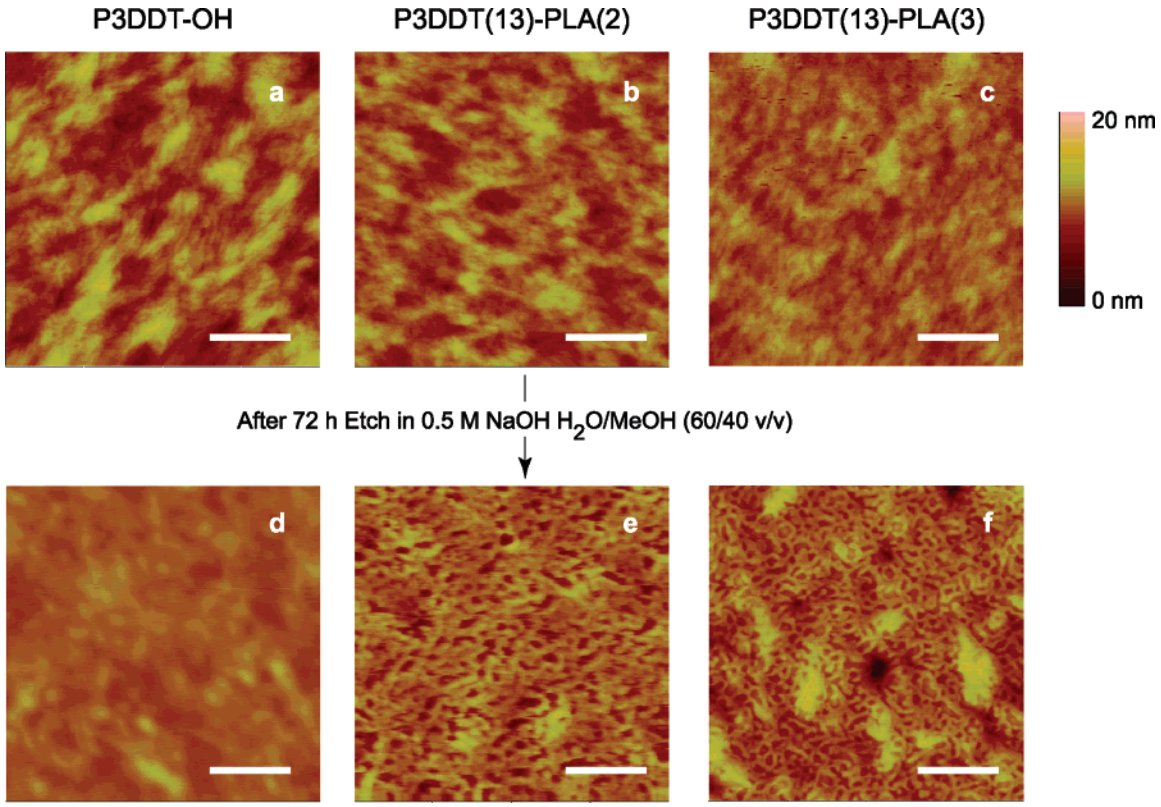

Figure 9. Tapping mode AFM height images of thin films of (a) P3DDT-OH, (b) P3DDT(13)-PLA(2), and (c) P3DDT(13)-PLA(3) prior to etching and (d) P3DDT-OH, (e) P3DDT(13)-PLA(2), and (f) P3DDT(13)-PLA(3) after exposure to an alkaline solution. Scale bars represent 250 nm.

matrix intact (Figure 8c). ^{1}H NMR experiments on both the P3DDT(13)-PLA(2) and P3DDT(13)-PLA(3) etched block copolymer films show that ~45% of the PLA is removed after 72 h of etching in the 0.5 M NaOH in water/methanol (60/40 v/v) bath. This amount of residual PLA was as low as we could achieve given the current etching technique. We believe that removal of PLA could be increased by increasing mass transport either by convective or diffusive means. While there is a residual amount of PLA left in the pitted block copolymer film (see next section), we have previously shown that having even a much larger amount of insulating material (greater than 40 wt %) has only a small effect on charge generation and conduction when incorporated into the active layer of blended bulk heterojunction organic photovoltaic (OPV) cells with a soluble fullerene.[90] The alkaline etching times used in these experiments suggest that P3DDT preferentially wets the ITO substrate since the films are remarkably stable in the etching bath for multiple days. The formation of a selective monolayer has been observed in other PLA block copolymer systems and varies based upon the substrate and surface treatment conditions.[57] We have observed similar block copolymer films dewet from other substrates over the course of much shorter etching periods.

Thin Film Imaging. In order to observe the morphology of the block copolymer films atomic force microscopy (AFM) was employed in tapping mode in order to minimize damage to the soft materials. Prior to etching, the homopolymer and block copolymer thin films show little change in surface height across the scan area of the microscope image (Figure 9, parts a−c). After placing the films in the etching bath for 72 h, the P3DDT-OH remains a smooth film intact with no apparent surface pitting (Figure 9d). On the other hand, the block copolymer films show discrete pits in the P3DDT matrices (Figure 9, parts e and f). In both the P3DDT(13)-PLA(2) and P3DDT(13)-PLA(3) polymers the pits in the films are irregularly shaped with characteristic "diameters" on the order of 35 ± 15 nm and depths of 8 ± 2 nm. We note that the pits may have larger depths than we report and that accurate measurements might be limited by the resolution of the tip of the microscope. Assuming the pits to be cylindrical in nature and 8 nm in depth, the increase in surface area of the pitted structures over the original planar structures is 47%. Phase separation may be dominated by P3DDT crystallization as opposed to the amorphous coil-*b*-coil systems where microphase separation is dominated by enthalpic interactions between the constituent monomers. Accordingly, the PLA must fill space not occupied by the crystalline domains of the P3DDT. This leads to pits with various diameters and geometries upon etching of the PLA. This type of phase separation has been seen in other P3AT block copolymer systems where polythiophene is the majority phase.[47]

Summary

We have shown the synthesis and molecular characterization of a new series of semiconducting-*b*-insulating block copolymers, P3AT-PLA, via two controlled polymerization steps. After exploring the thermal properties of these materials, we find that there is an advantage, in terms of processability, in using poly(3-dodecylthiophene) as the semiconducting moiety. By using the polymer with the longer alkyl side chain, we find a reduced melting point and, thus, as evidenced by DSC and TGA, annealing can be performed at temperatures lower than the degradation temperature of PLA. WAXS and DSC data shows that the lamellae structure of bulk P3DDT is maintained with the addition of PLA segments but the overall crystallinity of the polymers is slightly reduced as the amount of PLA present is increased. The materials are easily dissolved in a variety of organic solvents and were spun-cast from a high boiling point solvent in order to generate thin films with a high degree of P3DDT ordering. After etching the P3DDT-PLA thin films with

a gentle alkaline bath, we find pitted domains on the nanoscale where the PLA has been selectively removed without affecting the P3DDT crystalline structure as evidenced by AFM, ^{1}H NMR spectroscopy, and UV−vis absorption experiments. The facile synthesis and easy processability of these block copolymers leads to pitted films, which could be incorporated into a variety of organic electronic devices in order to improve performance. Two examples include greater sensitivity in VOC detection devices due to higher surface area for VOC−P3DDT interaction and improved contact between electron-donating and accepting materials in OPVs.

Acknowledgment. This work was funded by the Initiative for Renewable Energy and the Environment (IREE) at the University of Minnesota and the Xcel Energy Renewable Development Fund. Parts of this work were carried out in the University of Minnesota IT Characterization Facility, which receives partial support from the NSF through the NNIN program. We thank Ryan Wold for help with WAXS data collection and Dr. Rajeswari M. Kasi and Derek M. Stevens for helpful discussions.

References and Notes

(1) Skotheim, T.; Reynolds, J.; Elsembauer, R. *Handbook of Conducting Polymers*; Marcel Dekker: New York, 1998.
(2) Nalwa, H. S. *Handbook of Organic Conductive Molecules and Polymers*; J. Wiley & Sons: New York, 1996.
(3) McCullough, R. D. *Adv. Mater.* **1998**, *10*, 93−116.
(4) Wang, G.; Swensen, J.; Moses, D.; Heeger, A. J. *J. Appl. Phys.* **2003**, *93*, 6137−6141.
(5) Sirringhaus, H. *Adv. Mater.* **2005**, *17*, 2411−2425.
(6) Panzer, M. J.; Frisbie, C. D. *Adv. Funct. Mater.* **2006**, *16*, 1051−1056.
(7) Li, B.; Sauvé, G.; Iovu, M. C.; Jeffries-EL, M.; Zhang, R.; Cooper, J.; Santhanam, S.; Schultz, L.; Revelli, J. C.; Kusne, A. G.; Kowlewski, T.; Snyder, J. L.; Weiss, L. E.; Fedder, G. K.; McCullough, R. D.; Lambeth, D. N. *Nano Lett.* **2006**, *6*, 1598−1602.
(8) McQuade, D. T.; Pullen, A. E.; Swager, T. M. *Chem. Rev.* **2000**, *100*, 2537−2574.
(9) Padinger, F.; Rittberger, R. S.; Sariciftci, N. S. *Adv. Funct. Mater.* **2003**, *13*, 85−88.
(10) Reyes-Reyes, M.; Kim, K.; Carroll, D. L. *Appl. Phys. Lett.* **2005**, *87*, 083506.
(11) Li, G.; Shrotriya, V.; Huang, J.; Yao, Y.; Moriarty, T.; Emery, K.; Yang, Y. *Nat. Mater.* **2005**, *4*, 864−868.
(12) Kim, J. Y.; Lee, K.; Coates, N. E.; Moses, D.; Nguyen, T.; Dante, M.; Heeger, A. J. *Science* **2007**, *317*, 222−225.
(13) Sun, S.; Sariciftci, N. S. *Organic Photovoltaics: Mechanisms, Materials, and Devices*; Taylor & Francis: Boca Raton, FL, 2005.
(14) Janssen, R. A. J.; Hummelen, J. C.; Sariciftci, N. S. *MRS Bull.* **2005**, *30*, 33−36.
(15) Brabec, C. J.; Hauch, J. A.; Schilinsky, P.; Waldauf, C. *MRS Bull.* **2005**, *30*, 50−52.
(16) Chirvase, D.; Parisi, J.; Hummelen, J. C.; Dyakonov, V. *Nanotechnology* **2004**, *15*, 1317−1323.
(17) Zhang, R.; Li, B.; Iovu, M. C.; Jeffries-EL, M.; Sauvé, G.; Cooper, J.; Jia, S.; Tristram-Nagle, S.; Smilgies, D. M.; Lambeth, D. N.; McCullough, R. D.; Kowalewski, T. *J. Am. Chem. Soc.* **2006**, *128*, 3480−3481.
(18) Bates, F. S.; Fredrickson, G. H. *Annu. Rev. Phys. Chem.* **1990**, *41*, 525−557.
(19) Shull, K. R. *Macromolecules* **1992**, *25*, 2122−2133.
(20) Alexander-Katz, A.; Fredrickson, G. H. *Macromolecules* **2007**, *40*, 4075−4087.
(21) Russell, T. P.; Coulon, G.; Deline, V. R.; Miller, D. C. *Macromolecules* **1989**, *22*, 4600−4606.
(22) Menelle, A.; Russell, T. P.; Anastasiadis, S. H.; Satija, S. K.; Majkrzak, C. F. *Phys. Rev. Lett.* **1992**, *68*, 67−70.
(23) Sikka, M.; Singh, N.; Karim, A.; Bates, F. S.; Satija, S. K.; Majkrzak, C. F. *Phys. Rev. Lett.* **1993**, *70*, 307−310.
(24) Morkved, T. L.; Lu, M.; Urbas, A. M.; Ehrichs, E. E.; Jaeger, H. M.; Mansky, P.; Russell, T. P. *Science* **1996**, *273*, 931−933.
(25) Huang, E.; Rockford, L.; Russell, T. P.; Hawker, C. J. *Nature (London)* **1998**, *31*, 757−758.
(26) Hiemenz, P. C.; Lodge, T. P. *Polymer Chemistry*; CRC Press: Boca Raton, FL, 2007.
(27) Hillmyer, M. A. *Adv. Polym. Sci.* **2005**, *190*, 137−181.
(28) Halperin, A. *Macromolecules* **1990**, *23*, 2724−2731.
(29) Williams, D. R. M.; Fredrickson, G. H. *Macromolecules* **1992**, *25*, 3561−3568.
(30) Matsen, M. W.; Barrett, C. *J. Chem. Phys.* **1998**, *109*, 4108−4118.
(31) Radzilowski, L. H.; Wu, J. L.; Stupp, S. I. *Macromolecules* **1993**, *26*, 879−882.
(32) Chen, J. T.; Thomas, E. L.; Ober, C. K.; Hwang, S. S. *Macromolecules* **1995**, *28*, 1688−1697.
(33) Chen, J. T.; Thomas, E. L.; Ober, C. K.; Mao, G. P. *Science* **1996**, *273*, 343−346.
(34) Park, J.; Thomas, E. L. *Macromolecules* **2004**, *37*, 3532−3535.
(35) Jenekhe, S. A.; Chen, X. L. *Science* **1999**, *283*, 372−375.
(36) Jenekhe, S. A.; Chen, X. L. *J. Phys. Chem. B* **2000**, *104*, 6332−6335.
(37) Chen, X. L.; Jenekhe, S. A. *Macromolecules* **2000**, *33*, 4610−4612.
(38) de boer, B.; Stalmach, U.; van Hutten, P. F.; Melzer, C.; Krasnikov, V. V.; Hadziioannou, G. *Polymer* **2001**, *42*, 9097−9109.
(39) de Boer, B.; Stalmach, U.; Nijland, H.; Hadziioannou, G. *Adv. Mater.* **2000**, *12*, 1581−1583.
(40) Hadziioannou, G. *MRS Bull.* **2002**, *27*, 456−460.
(41) van der Veen, M. H.; de Boer, B.; Stalmach, U.; van de Wetering, K. I.; Hadziioannou, G. *Macromolecules* **2004**, *37*, 3673−3684.
(42) Olsen, B. D.; Segalman, R. A. *Macromolecules* **2005**, *38*, 10127−10137.
(43) Olsen, B. D.; Segalman, R. A. *Macromolecules* **2006**, *39*, 7078−7083.
(44) Olsen, B. D.; Li, X.; Wang, J.; Segalman, R. A. *Macromolecules* **2007**, *40*, 3287−3295.
(45) Sauvé, G.; McCullough, R. D. *Adv. Mater.* **2007**, *19*, 1822−1825.
(46) Iovu, M. C.; Craley, R.; Jeffries-EL, M.; Krankowski, A. B.; Zhang, R.; Kowalewski, T.; McCullough, R. D. *Macromolecules* **2007**, *40*, 4733−4735.
(47) Dai, C.; Yen, W.; Lee, Y.; Ho, C.; Su, W. *J. Am. Chem. Soc.* **2007**, *129*, 11036−11038.
(48) Jeffries-EL, M.; Sauvé, G.; McCullough, R. D. *Macromolecules* **2005**, *38*, 10346−10352.
(49) Hotta, S.; Rughooputh, S. D. D. V.; Heeger, A. J.; Wudl, F. *Macromolecules* **1987**, *20*, 212−215.
(50) Sugimoto, R.; Takeda, S.; Gu, H. B.; Yoshino, K. *Chem. Expr.* **1986**, *1*, 635−638.
(51) Hotta, S.; Soga, M.; Sonoda, N. *Synth. Met.* **1988**, *26*, 267−279.
(52) Loewe, R. S.; Khersonksky, S. M.; McCullough, R. D. *Adv. Mater.* **1999**, *11*, 250−253.
(53) Jeffries-EL, M.; Sauvé, G.; McCullough, R. D. *Adv. Mater.* **2004**, *16*, 1017−1019.
(54) Iovu, M. C.; Jeffries-EL, M.; Sheina, E. E.; Cooper, J. R.; McCullough, R. D. *Polymer* **2005**, *46*, 8582−8586.
(55) Iovu, M. C.; Jeffries-EL, M.; Zhang, R.; Kowalewski, T.; McCullough, R. D. *J. Macromol. Sci. A* **2006**, *43*, 1991−2000.
(56) Liu, J.; Sheina, E.; Kowalewski, T.; McCullough, R. D. *Agnew. Chem. Int. Ed.* **2002**, *41*, 329−332.
(57) Olayo-Valles, R.; Guo, S.; Lund, M. S.; Leighton, C.; Hillmyer, M. A. *Macromolecules* **2005**, *38*, 10101−10108.
(58) Mao, H.; Hillmyer, M. A. *Soft Matter* **2006**, *2*, 57−59.
(59) Ha, J.; Hillmyer, M. A.; Ward, M. D. *J. Phys. Chem. B* **2005**, *109*, 1392−1399.
(60) Olayo-Valles, R.; Lund, M. S.; Leighton, C.; Hillmyer, M. A. *J. Mater. Chem.* **2004**, *14*, 2729−2731.
(61) Kubo, T.; Parker, J. S.; Hillmyer, M. A.; Leighton, C. *Appl. Phys. Lett.* **2007**, *90*, 233113.
(62) Schmidt, S. C.; Hillmyer, M. A. *Macromolecules* **1999**, *32*, 4794−4801.
(63) Kricheldorf, H.; Berl, M.; Scharnagle, N. *Macromolecules* **1988**, *21*, 286−293.
(64) Wang, Y.; Hillmyer, M. A. *Macromolecules* **2000**, *33*, 7395−7403.
(65) Coakley, K. M.; Liu, Y.; Goh, C.; McGehee, M. D. *MRS Bull.* **2005**, *30*, 37−40.
(66) Olson, D. C.; Piris, J.; Collins, R. T.; Shaheen, S. E.; Ginley, D. S. *Thin Solid Films* **2006**, *496*, 26−29.
(67) Tashiro, K.; Kobayashi, M.; Kawai, T.; Yoshino, K. *Polymer* **1997**, *38*, 2867−2879.
(68) Zalusky, A. S.; Olayo-Valles, R.; Wolf, J. H.; Hillmyer, M. A. *J. Am. Chem. Soc.* **2002**, *124*, 12761−12773.
(69) Trznadel, M.; Pron, A.; Zagorska, M.; Chrzaszcz, R.; Pielichowski, J. *Macromolecules* **1998**, *31*, 5051−5058.
(70) Merlo, J. A.; Frisbie, C. D. *J. Phys. Chem. B* **2004**, *108*, 19169−19179.
(71) Iovu, M. C.; Sheina, E. E.; Gil, R. R.; McCullough, R. D. *Macromolecules* **2005**, *38*, 8649−8656.
(72) Li, S. J. *Biomed. Mater. Res.* **1999**, *48*, 342−353.
(73) Liu, J.; Loewe, R. S.; McCullough, R. D. *Macromolecules* **1999**, *32*, 5777−5785.
(74) Fan, Y.; Chen, G.; Tanaka, J.; Tateishi, T. *Biomacromolecules* **2005**, *6*, 3051−3056.

(75) Dubois, Ph.; Jacobs, C.; Jérôme, R.; Teyssié, Ph. *Macromolecules* **1991**, *24*, 2266−2270.
(76) Kuila, B. K.; Nandi, A. K. *Macromolecules* **2004**, *37*, 8577−8584.
(77) Miyauchi, S.; Kondo, T.; Oshima, K.; Yamauchi, T.; Shimomura, M.; Mitomo, H. *J. Appl. Polym. Sci.* **2000**, *77*, 3069−3076.
(78) Anderson, K. S.; Hillmyer, M. A. *Polymer* **2006**, *47*, 2030−2035.
(79) Malik, S.; Nandi, A. K. *J. Polym. Sci. B* **2002**, *40*, 2073−2085.
(80) Yang, C.; Orfino, F. P.; Holdcroft, S. *Macromolecules* **1996**, *29*, 6510−6517.
(81) Gurau, M. C.; Delongchamp, D. M.; Vogel, B. M.; Lin, E. K.; Fischer, D. A.; Sambasivan, S.; Richter, L. J. *Langmuir* **2007**, *23*, 834−842.
(82) Causin, V.; Marega, C.; Marigo, A.; Valentini, L.; Kenny, J. M. *Macromolecules* **2005**, *38*, 409−415.
(83) Zhao, Y.; Keroack, D.; Yuan, G.; Massicotte, A. *Macromol. Chem. Phys.* **1997**, *198*, 1035−1049.
(84) Liu, S. L.; Chung, T. S. *Polymer* **2000**, *41*, 2781−2793.
(85) Park, Y. D.; Kim, D. H.; Jang, Y.; Cho, J. H.; Hwang, M.; Lee, H. S.; Lim, J. A.; Cho, K. *Org. Electron.* **2006**, *7*, 514−520.
(86) Babel, A.; Jenekhe, S. A. *Synth. Met.* **2005**, *148*, 169−173.
(87) Chen, S.; Lee, S. *Polymer* **1995**, *36*, 1719−1723.
(88) Prosa, T. J.; Moulton, J.; Heeger, A. J.; Winokur, M. J. *Macromolecules* **1999**, *32*, 4000−4009.
(89) Sunderberg, M.; Inganäs, O.; Stafström, S.; Gustafsson, G.; Sjögren, B. *Solid State Commun.* **1989**, *71*, 435−439.
(90) Boudouris, B. W.; Kasi, R. M.; Frisbie, C. D.; Hillmyer, M. A. *PMSE Prepr.* **2006**, *95*, 103.

MA071626D